Journal of Materials Chemistry B

Accepted Manuscript

ROYAL SOCIETY OF CHEMISTRY

www.rsc.org/materialsB

Electrochemical Immunosensor for Simultaneous point-of-care Cancer markers Based on Host-Guest Inclusion of β-cyclodextrin-Graphene oxide

Taotao Feng,[a] Xiuwen Qiao*,[a] Haining Wang,[a] Zhao Sun,[a] Yu Qi*,[a] Chenglin Hong*[a,b]

[a] School of Chemistry and Chemical Engineering, Shihezi University, Shihezi 832003, PR China

[b] Key Laboratory for Green Processing of Chemical Engineering of Xinjiang Bingtuan, Engineering Research Center of Materials-Oriented Chemical Engineering of Xinjiang Production and Construction Corps, Key Laboratory of Materials-Oriented Chemical Engineering of Xinjiang Uygur Autonomous Region, Shihezi 832003, PR China

*Corresponding author:

Tel.: +86-18097586568. Fax: +86-993-2057270.

E-mail: hcl_tea@shzu.edu.cn (Chenglin Hong).

qxw_tea@shzu.edu.cn (Xiuwen Qiao).

qy01_tea@shzu.edu.cn (Yu Qi).

Abstract

A novel electrochemical immunosensor was developed for the simultaneous detection of alpha-fetoprotein (AFP) and carcinoembryonic antigen (CEA) using Cu_2O-graphene oxide-β-cyclodextrin (Cu_2O-GO-CD) and β-cyclodextrin-graphene oxide-ferrocenecarboxylic acid (GO-CD-Fc-COOH) as the distinguishable signal probe, and gold nanoparticles-graphene oxide (GO-AuNPs) as the sensor platform. The GO-CD displayed the excellent solubility in water and rich capture capability to the Fc-COOH and the secondary antibody. The proposed immunosensor exhibited an excellent electrochemical performance. The linear ranges were from 0.001 $ng \cdot mL^{-1}$ to 80 $ng \cdot mL^{-1}$ for AFP and CEA with the detection limit 0.0002 $ng \cdot mL^{-1}$ for AFP and 0.0001 $ng \cdot mL^{-1}$ for CEA. With the merits of acceptable stability, high sensitivity, wide linear range and low detection limit, the proposed immunosensors showed great potential for the simultaneous detection of multi-analyte in the clinical diagnostics.

Keywords: Host-Guest Interaction, β-cyclodextrin, Simultaneous point-of-care, Immunosensors, Cancer markers

Introduction

The 《Global Cancer Report 2014》 that published by the World Health Organization points, the most common cancers diagnosed as the lung, breast, and large bowel in the whole world in 2012, and the leading causes of cancer death were the lung, liver, and stomach cancer. The early detection and screening of cancer markers, as an effective means to prevent and treat the cancer, had been widely used in the clinical diagnosis. Recently, various analytical methods were developed for assay of single tumor marker. However, in the clinical diagnosis, the detection of single tumor marker is frequently criticized for the high rate of false positives and negatives,[1] because no single tumor marker is sensitive and specific to a particular tumor.[2,3] To address this, the simultaneous detection of two or more tumor makers have shown a growing demand in the clinical diagnosis and the screening of cancer markers, because of higher diagnostic specificity and the more reliable datum to a type of cancer.[4] At present, a variety of analytical strategies and methods were performed for the simultaneous detection of the multiple cancer markers. Among them, the electrochemical immunoassay could be selected as a one of the leading trends due to its high sensitivity and portability.[5-7]

In the simultaneous multi-analyte electrochemical detection, the multiple label and the spatial resolution strategies are two dominant modes to build an electrochemical immunosensor for the simultaneous detection of the multiple cancer markers in the reported literature.[8-10] One of the most popular ways of a multiplex assay is use the carriers with some distinguishable signal probe to identify the different target tumor marker. The mode usually necessitates the sandwich assay format and the redox-probe of generating signals at different potentials, where antigens were specifically bound to their primary antibodies on electrode surface, and then the labeled secondary antibody are selectively identified. Thereby, the electrochemical immunosensor would generate distinct signals with the characteristic peak potentials.

Graphene and graphene oxide (GO), a single layer of sp^2-hybridized carbon

atoms in a two-dimensional (2D) honeycomb lattice,[11] is usually used to develop the promising nano-carrier in the electrochemical sensors because of its large specific surface area, thermal properties, strong mechanical strength, chemical stability and excellent conductivity.[12-15] To date, many attempts have been made to design and construct electrochemical biosensors based on the graphene. However, the graphene generally rends to form irreversible agglomerates through van der Waals forces, which leads to greatly technical difficulty in applications[16] that should be resolved by adding various dispersants. However, in most cases, the presence of dispersants in graphene composite perhaps were unwelcome for many technological applications, which usually result in poor properties.[17]

Recently, Gold nanoparticles (AuNPs) have been widely used to enhance the sensitivity of the electrochemical sensors substrate[18-22] due to its distinct physical and chemical attributes such as high surface-to-volume ratio, excellent electrical conductivity and biocompatibility. Thus, it is expected that more enhanced performances could be attained by incorporate of the AuNPs with GO. Since the incorporation of AuNPs and GO could provide the sufficient conductivity, large surface area and good biocompatibility.

β-cyclodextrin (CD) is toroidal in shape with a hydrophilic exterior surface and a hydrophobic interior cavity,[23,24] and holds great promise for potential applications in immunoassay. These interesting characteristics not only can enable them as the solubilizers to improve water-solubility and stability of the functional materials, but also has high molecular selectivity and enantioselectivity. Then, various organic and biological guest molecules could enter into their hydrophobic cavities to form stable host-guest inclusion complexes or nanostructure supra-molecular assemblies through various kinds of intermolecular interactions.[25-27] In recent years, the modification of CD on GO surfaces (GO-CD) by the strong hydrogen bonding as ideal nano-carrier has attracted enormous attentions in electrochemical sensors.[28,29] Because the GO-CD simultaneously possess two materials individual unique properties, such as large surface area and high conductivity of reduce graphene oxide (rGO), and rich capture capability and good water-soluble of CD.

As an excellent electron mediator, cuprous oxide (Cu_2O) have widely used for a stability adsorption on the GO surface. Ferrocene (Fc) and its derivatives is an excellent probe, it could generate stable redox states. It is often used as a protein biomarker or redox active species for biomolecules detection in electrochemical systems.[30] This two electron mediators have different characteristics peak potential that is very low, and provides favorable conditions for the simultaneous detection of two cancer markers. However, the leakage has been a main problem for the entrapment of Fc. In order to prevent the leakage of Fc, we turned our eyes to the supra-molecular host-guest recognition technology.[31] The Fc was captured on the GO-CD surface via the host-guest interaction between GO-CD and Fc. Hence, Cu_2O-GO and GO-CD-Fc were employed as the signal probes for the simultaneous detection of two cancer markers. To our best knowledge, there are no published data for application of GO-AuNPs as platform, and the GO-CD-Fc and the Cu_2O-GO-CD as the signal probes in the fabrication of electrochemical immunosensor for the simultaneous detection of two cancer markers.

Herein, we present a sandwich-type electrochemical immunosensor for the simultaneous detection of CEA and AFP using GO-CD-Fc-anti-CEA and Cu_2O-GO-CD-anti-AFP as the distinguishable signal probes, and the GO-AuNPs as the sensor platform. The proposed electrochemical immunosensor has exhibited excellent performances for the simultaneous detection of CEA and AFP. The main advantages of the immunosensor contribute to several aspects as following: (i) the GO-AuNPs could immobilize lots of primary antibodies without denaturation, (ii) a large of CD were immobilized on the GO surface that could overcome the aggregation of reduce graphene oxide, and form a host to capture a redox label and antibody, (iii) the simultaneous detection of CEA and AFP could provide a very efficient data for the diagnosis and early detection of cancer. Moreover, the prepared method was applied to detect CEA and AFP in real blood or tissue samples.

Experimental

Synthesis of immunosensing probes

The GO-CD was prepared according to the previous method.[23] Briefly, 10 mL of 0.5 $mg \cdot mL^{-1}$ homogeneous GO, 10 mL of 80 $mg \cdot mL^{-1}$ CD and 150 μL of $NH_3 \cdot H_2O$ were mixed by ultrasonication. Then, 8 μL of hydrazine solution was added to the solution under magnetic stirring at 60℃ for 4 h. A stable black dispersion was obtained and filtered with a membrane (0.22 μm) to obtain the GO-CD. Next, 1 mg of GO-CD and 2 mg of Fc-COOH were added in 10 mL ethanol, and then strongly stirring for 24 h at room temperature. After filtrating, the residual Fc has been removed, and the GO-CD-Fc-COOH host-guest inclusion complexes were obtained. Subsequently, 200 μL of 10 $\mu g \cdot mL^{-1}$ secondary anti-CEA was added into 1 mL of 0.5 $mg \cdot mL^{-1}$ activated GO-CD-Fc-COOH solution and gently stirred for 12 h at 4℃. Using EDC/NHS as the coupling agents, the anti-CEA were covalently immobilized onto the GO-CD-Fc-COOH via amide bond formation between the -COOH of Fc-COOH and the amine groups of the anti-CEA. The obtained probe was incubated in BSA for 2 h. Finally, the obtained GO-CD-Fc-anti-CEA was re-dispersed in 1 mL of PBS.

The Cu_2O-GO was synthesized according to the modified previously reported procedures. Firstly, 6.92 mL of 0.3 $mg \cdot mL^{-1}$ GO, 0.5 mL of 0.1 M $CuCl_2$ and 0.087 g of SDS was mixed under vigorous magnetic stirring in a water bath at 32~34℃. Then, 0.18 mL of 1.0 M NaOH solution was introduced and the $Cu(OH)_2$ precipitate formed. Next, 2.40 mL of 0.1 M $NH_2OH \cdot HCl$ was injected into the solution (5 s) and stirred for 20 s, and then the Cu_2O nanocrystals were allowed to grow for 60 min. Finally, the product was centrifuged and washed with the mixture of a 1:1 (v/v) of water and ethanol. The Cu_2O-GO-CD was synthesized using the above method under isolation oxygen atmosphere.The purified precipitate was finally dispersed in ethanol at 4℃. The anti-AFP and 1 mg of 0.5 $mg \cdot mL^{-1}$ Cu_2O-GO-CD was mixed for 12 h at 4℃. The obtained Cu_2O-GO-CD-anti-AFP was re-dispersed in 1 ml of PBS (pH 7.4) and stored at 4℃ before use.

Assembly of the immunosensor

Before assembly, the bare glassy carbon electrode (GCE, 4 mm diameter) was polished with 0.5 μm and 50 nm alumina slurry, until a mirror-like surface was

acquired, and then sonicated in ethanol and deionized water and dried. Subsequently, 10 μL of GO-AuNPs was placed onto the GCE surface and dried. Then, the modified electrode was incubated in 200 $\mu g \cdot mL^{-1}$ primary anti-AFP and anti-CEA solution at 4℃ for 12 h. In order to block the remaining active sites, the electrode was incubated in a BSA for 1 h. Next, the modified electrode was incubated in a series of the same concentration of AFP and CEA for 40 min at room temperature. The fabrication process of the immunosensor and the preparation of immunosensing probes were illustrated in Scheme 1.

<Scheme 1>

Immunoassay protocol and electrochemical measurement

Based on the sandwich-type immunosensor, the GCE/GO-AuNPs/Ab_1/antigen electrode was incubated with Ab_2 bioconjugates for 40 min at room temperature to form probe-Ab_2/CEA/Ab_1 format. The responses of the above modified electrode was done for the simultaneous measurement of AFP and CEA in 0.1 M PBS (pH 7.4) solution containing 0.1 M KCl by differential pulse voltammetry (DPV) at a potential window of -0.6 to +0.6 V at room temperature. The two distinguishable oxidation peaks was appeared, each peak indicated one target analyte and the peak current responses was quantitative correlative with their concentration respectively. Therefore, the changes of electrochemical responses signal reflected the concentration changes of CEA and AFP directly.

Results and discussion

Characterization of the GO-CD-Fc

The morphology of GO and GO-CD was observed by TEM. The morphology of GO was homogeneous and quite smooth, and there was a little wrinkles and like transparent silk fabrics (Fig. 1A). Whereas, the surface of GO-CD was rough, and there are more wrinkles and folds rather than the GO, and the contrast was apparently increased (Fig. 1B). The FT-IR of GO, GO-CD and GO-CD-Fc-COOH are shown in Fig. 1D. The FT-IR of GO (a) shows a typical peak at 1731 cm^{-1}, 1400 cm^{-1}, 1221 cm^{-1}, 1059 cm^{-1} and 1540 cm^{-1}, due to the C=O group, carboxyl C–O, epoxy C–O,

alkoxy C–O and C=C, respectively, which indicates that there are large amounts of oxygen-containing functional groups on the GO surface. However, the peak intensity at 1731 cm^{-1} of carbonyl C=O was disappeared (c), and the peaks intensity at 1400 cm^{-1}, 1221 cm^{-1} and 1059 cm^{-1} of GO correspond to the all C-O functional groups greatly decreased dramatically except the C=C conjugation (1580 cm^{-1}). A typical CD absorption features (c) at 579 cm^{-1}, 708 cm^{-1}, 757 cm^{-1}, 944 cm^{-1} indicates the ring vibrations, and the coupled C-O/C-C stretching/O-H bending vibrations at 1028 cm^{-1} and 1076 cm^{-1}, the coupled C-O-C stretching/O-H bending vibrations at 1157 cm^{-1}, and -CH_2- stretching vibrations at 2924 cm^{-1}, which were clearly confirmed that the CD molecules are successfully attached to the surface of GO. After GO-CD reacting with Fc-COOH, the spectrum of the GO-CD-Fc-COOH (d) shown the characteristic peak at 1680 cm^{-1} increased by comparison with GO-CD. A broad characteristic peak at ~3500 cm^{-1} indicate -COOH group, which were the result of bonding between the hydrophobic interior cavity of CD and cyclopentadiene of Fc-COOH, and a new absorption bands at about 480 cm^{-1} (Fe-Cp) appeared (e). This indicated the successful formation of GO-CD-Fc-COOH.

Characterization of the Cu_2O-GO-CD

The TEM was used to verify the formation of Cu_2O-GO hybrid. A homogeneous Cu_2O nanoparticles (diameters 100-150 nm) are attached on the surface of GO (Fig. 1C). No aggregation of GO sheets and free Cu_2O was observed. The structural characterization of the GO and Cu_2O-GO were also performed by the XRD (Fig.S2). The FT-IR of Cu_2O, Cu_2O-GO and Cu_2O-GO-CD were shown in Fig. 1E. The intense absorption band at 624 cm^{-1} is assigned to the Cu (I)-O stretching vibration (curve a). A typical GO absorption features (curve b) at 1530 cm^{-1} (C=C conjugation) and 1714 cm^{-1} (C=O group) were emerged when the Cu_2O was supported GO (curve b). Whereas the FT-IR of Cu_2O-GO-CD (curve c) exhibits the typical CD absorption features peak of the ring vibrations at 702 cm^{-1}, 758 cm^{-1}, and 941 cm^{-1}, and the coupled C-O-C stretching/OH bending vibrations at 1151 cm^{-1} and the -CH_2- stretching vibrations at 2925 cm^{-1} that could clearly confirm the CD molecules are

attached to the surface of Cu_2O-GO successfully.

<Figure 1>

Advantages and characterization of electrochemical immunosensor

The capture capability and the enrichment functions of CD are very important to improve the electrochemical performances. To demonstrate the capture capability and enrichment functions of CD, the electrochemical behaviors of the modified electrode were investigated. As shown in Fig. 2A, the peak current of GCE/GO-CD-Fc (curve d) shows a remarkable increase relative to the peak currents of the GCE/GO-Fc (curve c), which indicates the GO-CD have a favorable capture capability and enrichment functions to electron mediator Fc than GO. While, no redox peaks were observed at bare GCE electrode (curve a) and GCE/GO (curve b) electrode that is attributed to absent of electron mediator Fc on the surface of the modified electrode. Fig. 2B showed the peak currents of the GCE, GCE/GO, GCE/GO-biomolecules and GCE/GO-CD-biomolecules electrodes in 5 mM $[Fe(CN)_6]^{3-/4-}$ containing 0.1 M KCl. A pair of distinct redox peaks were observed at a bare GCE electrode (curve a) while the peak current of GCE/rGO was sharply increased (curve b) due to its excellent electrical conductivity. After the electrode was modified with the GCE/rGO-biomolecules, the peak current of the electrode decreased (curve c) because of biomolecules blocked the electron transfer of $[Fe(CN)_6]^{3-/4-}$. The peak current of GCE/GO-CD-biomolecules (curve d) electrode showed a significantly decrease relative to the peak currents of the GCE/GO-biomolecules electrode because the GCE/GO-CD have stronger capture capability to biomolecules that can further hinder the electron transfer. The results indicate that the GO-CD has a favorable capture capability and enrichment functions to biomolecules than GO. All the results suggest that the GO-CD not only shows the excellent properties of GO but also exhibits the excellent capture capability and enrichment functions of CD to Fc and biomolecules.

<Figure 2>

As the redox probes of electrochemical immunosensor, the Cu_2O-GO-CD and GO-CD-Fc were produced by introducing the Cu_2O and Fc-COOH into the GO-CD

via an electrostatic interaction between Cu_2O and GO and host-guest interaction between the Fc-COOH and the CD, respectively. Then, the secondary antibodies -AFP and -CEA were connected to the redox probes. Herein, the CD plays three roles: (1) as a solubilizers, to make graphene more hydrophilic and improve the solubility and stability of graphene in water (2) a large number of CDs were supported on the surface of GO that they could develop molecular recognition and enrich functions of GO more effectively (3) providing a cavity for the further interaction with Fc and secondary anti-AFP without denaturation. Additional, the GO-AuNPs has a large specific surface area and the active sites capable of immobilizing primary antibodies. As a result, the GO-CD was utilized to produce the substrate and the GO-AuNPs was utilized to build the sensor platform with high sensitivity. With the sandwich-type assay format, the antigen-antibody immune-complex was formed on the surface of the GCE/GO-AuNPs electrode. The electrochemical signals could be obtained simultaneously at the peak potentials of Cu_2O and Fc. The peak currents were dependent on the concentration of the corresponding antigens, respectively.

The cyclic voltammetry (CV) and electrochemical impedance spectroscopy (EIS) have been employed to characterize the surface properties of different modified electrodes (Fig.S3). The results demonstrated that the electrochemical immunosensor was fabricated successfully. Furthermore, the relationship between the scan rate and the peak current of AFP and CEA were also investigated. The results shows that the peak current increased with the increased of CV scanning rate (Fig.S4) and the peak current increased linearly with the square root of scan rate in the range of 20-300 $mV \cdot s^{-1}$ with the high co-efficient (inset of Fig. S4), which is consistent with diffusion controlled electrochemical reaction system.

Amplification effect of the electrochemical immunosensor

In order to verify the effect of each individual component, the (Cu_2O and Fc) and (Cu_2O-GO and Fc-GO) instead of (Cu_2O-GO-CD and GO-CD-Fc), AuNPs instead of GO-ANPs were used to fabricate the immunosensor probes and platform. The proposed immunosensor was assessed by contrasting the electrochemical signal of

four different immunosensors (Fig.S7). The first immunosensor was as the control experiment with a low electrochemical signal (curve a). Compared with the first immunosensor, the electrochemical signal of the second immunosensor (curve b) was improved 2.5-fold, because the graphene could accelerate the electron transfer, and provide a large surface area to support more AuNPs that could fix more primary antibodies. Compared with the second immunosensor, the third immunosensor signal was improved 2.4-fold indicated that graphene is an excellent nano-carrier due to its large specific surface area, excellent conductivity and electrocatalytic activity. However, compared with the second immunosensor, the fourth immunosensor signal was enhanced 4-fold after introducing CD. From the third immunosensor to the fourth immunosensor, the electrochemical signal was enhanced 1.7-fold which could be attributed to two reasons: (i) a large amount of CD was immobilized on the GO surface that increase water solubility of graphene, and (ii) GO-CD can be immobilized more mediator and secondary antibodies by host-guest interactions to increased sensitivity and stability of immunosensor.

Performance analysis of the immunoassay

Under the optimized conditions (Fig.S6), the analytical performances of the proposed multiplexed immunoassay were verified for the detection of AFP and CEA by DPV. As shown in Fig. 3A, the DPV peak currents of the multiplexed immunoassay increased with the increased of AFP and CEA concentrations in the range of 0.001~80 $ng \cdot mL^{-1}$. The two calibration plots displayed a good linear relationship between the peak currents and the logarithm of the analyte concentration in the ranges of 0.001~80 $ng \cdot mL^{-1}$ for AFP and CEA respectively (Fig. 3B, C). The correlation coefficients were 0.996 and 0.997, and the detection limits (S/N=3) were 0.0002 $ng \cdot mL^{-1}$ and 0.0001 $ng \cdot mL^{-1}$ for AFP and CEA, respectively. Besides, the obtained detection limits for AFP and CEA were lower than those of the previous multiplex assay methods. The comparison of the electrochemical performance between the proposed immunosensor and some recently published studies is listed in Table 1S.

<Figure 3>

Assess specificity, reproducibility and stability

The specificity is one of the crucial factors for electrochemical immunosensor in the clinical diagnosis. The specificity of the developed multiplexed immunoassay was tested by using some kinds of interferences such as BSA, HRP and DA. In order to obtain the peak currents response, the modified electrode was incubated in the mixture solution containing of 1.0 ng·mL^{-1} AFP, 1.0 ng·mL^{-1} CEA and 100 ng·mL^{-1} interference, and 1.0 ng·mL^{-1} AFP and 1.0 ng·mL^{-1} CEA without interference respectively (Fig.4). Compared with the current response obtained by incubated in the solution of 10 ng·mL^{-1} AFP and CEA, the variation in the current caused by the interfering substances was less than 4.8%, which indicated that BSA, HRP and DA could not interfere with the detection of AFP and CEA. Thus, the proposed immunosensor possesses good specificity for AFP and CEA.

As well all known, the reproducibility of electrochemical immunosensor also is a key factor in the practical application. The reproducibility of the proposed electrochemical immunosensor for simultaneous detection of AFP and CEA were investigated with the intra-assay and inter-assay precision by DPV. The intra-assay precision of the proposed electrochemical immunosensor was assessed by assaying two different concentration levels (0.1 ng·mL^{-1} and 10 ng·mL^{-1}) of CEA and AFP for 5 immunosensor arrays that made at the same batch and the relative standard deviation (RSD) were calculated as 3.2% and 4.1% for 0.1 ng·mL^{-1} AFP and CEA, 2.1% and 2.6% for 10 ng·mL^{-1} AFP and CEA, respectively. The inter-assay precision was assessed by detecting the same concentration of AFP and CEA with 5 immunosensor arrays that made at different batches and the RSD were calculated as 4.8% and 3.5% for 0.1 ng·mL^{-1} AFP and CEA, 3.8% and 3.1% for 10 ng·mL^{-1} AFP and CEA. The results indicated that the proposed immunosensor displayed good precision and reproducibility, which could be ascribed to the simplicity of the label. In addition, the stability of the immunosensor has also been studied. There are more than 89.6% of the initial responses (n=5, RSD=3.7%) has remained for both AFP and CEA after stored at 4℃ for 1 month. Consequently, the reproducibility and stability of the

proposed immunosensor was accepted.

<Figure 4>

Determination of clinical serum samples

The analytical applicability, reliability and validity of the proposed multiplexed electrochemical immunosensor were evaluated by assaying five clinical serum samples using a standard addition method, and compared to the enzyme-linked immunosorbent assay (ELISA) method. The results are listed in Table 1 and Table S2, respectively. Table 1 shows that the relative standard deviations were 2.1%~5.2% for AFP and 2.4%~4.6% for CEA and the recovery were 98.2%~103.2% for AFP and 98.2%~101.8% for CEA, respectively. Table 2S shows that the relative errors between the two methods were 2.6%~4.1% and 2.8%~4.8% for AFP and CEA, respectively. Therefore, the proposed immunosensor have the potential application for simultaneous determination of AFP and CEA in the clinical diagnostics.

Conclusions

In conclusion, a sensitive multiplexed electrochemical immunosensor was developed for the simultaneous detection of AFP and CEA using GO-AuNPs as sensor platform, the Cu_2O-GO-CD and GO-CD-Fc as the distinguishable signal probes. The GO-AuNPs could immobilize a large of primary antibodies without deactivation. As the solubilizers, CD not only can increase the water-solubility of graphene to prevent gathering, but also be capable of forming a host-guest inclusion complexes with redox probe and antibody to maintain the good activity. The GO-CD-tagged Cu_2O and Fc based on the multiplex assay method showed high sensitivity, wide linear range, very low detection limits, good accuracy negligible cross-talk, and acceptable detection selectivity and reproducibility, and acceptable stability, demonstrating the potential application in the clinical diagnostics and screening.

Acknowledgment

The authors are grateful for the National Natural Science Foundation of China (No. 21065009), the Key Project of Chinese Ministry of Education (No. 2010250) and Bingtuan Innovation Team in Key Areas (No.2015BD003).

References

1 F. Y. Kong, B. Y. Xu, Y. Du, J. J. Xu, H. Y. Chen, *Chem. Commun.*, 2013, **49**, 1052-1054.

2 Z. Yang, Y. Chevolot, T. Géhin, V. Dugas, N. Xanthopoulos, V. Laporte, T. Delair, Y. Ataman-Onal, G. Choquet-Kastylevsky, E. Souteyrand, E. Laurenceau, *Langmuir*, 2013, **29**, 1498-1509.

3 Y. Zhang, W. Liu, S. Ge, M. Yan, S. Wang, J. Yu, N. Li, X. Song, *Biosens. Bioelectron.*, 2013, **41**, 684-690.

4 N. Liu, Z. Liu, H. Han, Z. Ma, *J. Mater. Chem. B*, 2014, **2**, 3292-3298.

5 T. Feng, X. Qiao, H. Wang, Z. Sun, C. Hong, *Anal. Methods*, 2015, **7**, 10032-10039.

6 A. Mars, C. Paeolo, N. Raoua, K. Boujlel, A. Merkoci, *J. Mater. Chem. B*, 2013, **1**, 2951-1955.

7 B.V. Chikkaveeraiah, A. Bhirde, N.Y. Morgan, H.S. Eden, X. Chen, *ACS Nano*, 2012, **8**, 6546-6561.

8 S. Morais, L. A. Tortajada-Genaro, T. Arnandis-Chover, R. Puchades, A. Maquieira, *Anal. Chem.*, 2009, **81**, 5646.

9 J. Wang, X. Mi, H. Guan, X. Wang, Y. Wu, *Chem. Commun.*, 2011, **47**, 2940-2942.

10 Z. G. Yang, Y. Chevolot, Y. A. Onal, G. C. Kastylevsky, E. Laurenceau, *Sens. Actuators B*, 2012, **175**, 22-28.

11 G. Moon, Y. Park, W. Kim, W. Choi, *Carbon*, 2011, **49**, 3454-3462.

12 B. Konkena, S. Vasudevan, *Anal. Chem.*, 2013, **85**, 5114-5119.

13 M. J. Allen, V. C. Tung, L. Gomez, Z. Xu, L. M. Chen, K. S. Nelson, C. Zhou, R. B. Kaner, Y. Yang, *Adv. Mater.*, 2009, **21**, 2098-2102.

14 T. Feng, X. Qiao, H. Wang, Z. Sun, C. Hong, *Biosens. Bioelectron.*, 2016, 79, 48-54.

15 K.I. Bolotin, *Graphene*, 2014, **4**, 199-227.

16 H. P. Cong, X. C. Ren, P. Wang, S. H. Yu, *ACS nano*, 2012, **6**, 2693-2703.

17 Y. C. Si, E. T. Samulski, *Nano Lett.*, 2008, **8**, 1679-1682.

18 Y. Zhu, P. Chandra, Y. B. Shim, *Anal. Chem.*, 2012, **85**, 1058-1064.

19 U. H. F. Bunz, V. M. Rotello, *Angew. Chem., Int. Ed.*, 2010, **49**, 3268-3279.

20 X. Wang, Q. Han, N. Yu, J. Li, L. Yang, R. Yang, C. Wang, *J. Mater. Chem. B*, 2015, **3**, 4036-4042.

21 J. Li, Q. Han, X. Wang, N. Yu, L. Yang, R. Yang, C. Wang, *Small*, 2014, **10**, 4386-4394.

22 K. Saha, S. S. Agasti, C. Kim, X. Li, V. M. Rotello, *Chem. Rev.*, 2012, **112**, 2739−2779.

23 Y. Guo, S. Guo, J. Ren, Y. Zhai, S. Dong, E. Wang, *ACS Nano*, 2010, **4**, 4001-4010.

24 E. Zor, H. Bingol, A. Ramanaviciene, A. Ramanavicius, M. Ersoz, *Analyst*, 2015, **140**, 313-321.

25 F. Wang, M. G. Khaledi, *Anal. Chem.*, 1996, **68**, 3460-3467.

26 J. Liu, Y. Chen, Y. Guo, F. Yang, F. Cheng, *J. Nanomater.*, 2013, **2013**, 11.

27 Z. Zhang, S. Gu, Y. Ding, M. Shen, L. Jiang, *Biosens. Bioelectron.*, 2014, **57**, 239-244.

28 M. Chen, Y. Meng, W. Zhang, J. Zhou, J. Xie, G. Diao, *Electrochim. Acta*, 2013, **108**, 1-9.

29 Q. Han, Y. Wang, Y. Huang, L. Guo, Y. Fu, *Analyst*, 2013, **138**, 2051-2056.

30 J. Liu, S. Tian, L. Tiefenauer, P. E. Nielsen, W. Knoll, *Anal. Chem.*, 2005, **77**, 2756-2761.

31 L. S. Wang, J. P. Lei, R. N. Ma, H. X. Ju, *Anal. Chem.*, 2013, **85**, 6505-6510.

Scheme 1 The schematic of the sandwich-type electrochemical immunosensor.

Fig. 1 The TEM of GO (A), GO-β-CD (B), GO-Cu_2O (C). The FTIR (D) of GO (a), β-CD (b), GO-CD (c), GO-CD-Fc-COOH (d) and Fc-COOH (e). (E) The FT-IR of GO (a), Cu_2O-GO (b) and Cu_2O-GO-CD (c).

Fig. 2 CVs (A) of Fc at GCE electrode (curve a), GCE/GO electrode (curve b), GCE/GO-Fc electrode (curve c), and GCE/GO-CD-Fc electrode (curve d) in 0.1 M PBS (pH 7.4) containing 0.1 M KCl. CVs (B) of bare GCE (curve a), GCE/GO (curve b), GCE/GO-biomolecules (curve c) and GCE/GO-CD-biomolecules electrode (curve d) in 0.1 M PBS (pH 7.4) containing 0.1 M KCl and 5 mM $[Fe(CN)_6]^{3-/4-}$. Scan rate: 50 $mV \cdot s^{-1}$.

Fig. 3 DPV (A) of the modified electrodes towards different concentrations of CEA and AFP from 0 to 80 $ng \cdot mL^{-1}$ in 0.1 M PBS (pH 7.4) containing 0.1 M KCl under optimal conditions. Calibration plots of the current of the immunosensor toward different concentrations of CEA (B) and AFP (C). Error bar = SD (n=5).

Fig. 4 The peak response of the immunosensor to 1.0 $ng \cdot mL^{-1}$ AFP and CEA, 1.0 $ng \cdot mL^{-1}$ AFP and CEA + 100 $ng \cdot mL^{-1}$ BSA, 1.0 $ng \cdot mL^{-1}$ AFP and CEA + 100 $ng \cdot mL^{-1}$ DA, 1.0 $ng \cdot mL^{-1}$ AFP and CEA + 100 $ng \cdot mL^{-1}$ HRP. Above detections in 0.1 M PBS (pH 7.4) containing 0.1 M KCl. Error bar = SD.

Table 1 Recovery results for the detection of CEA and AFP in clinical serum samples by DPV in 0.1 M PBS containing 0.1 M KCl (pH 7.4) (n= 5).

Scheme 1

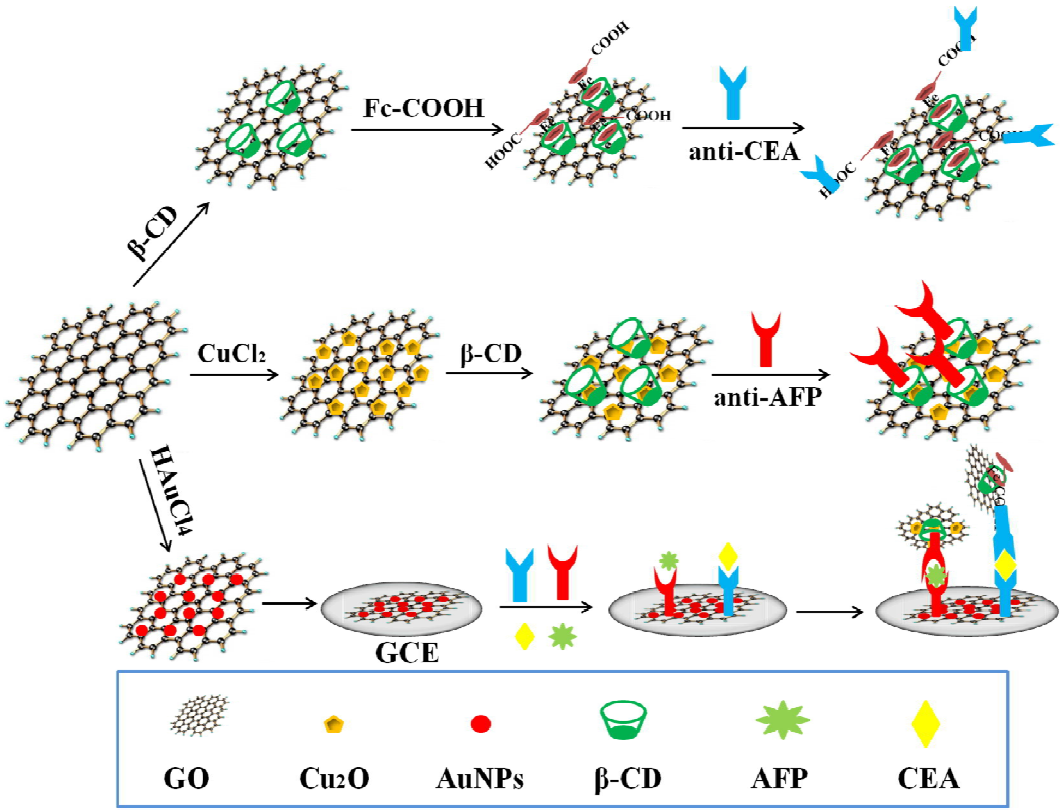

Fig. 1

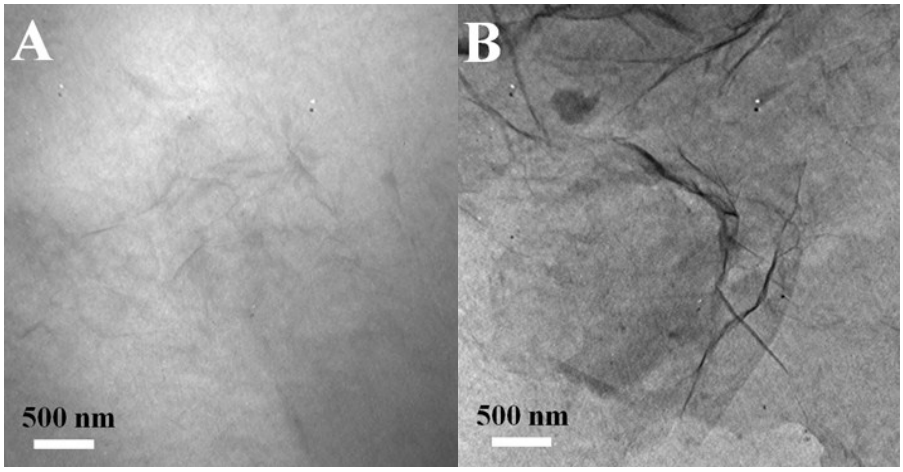

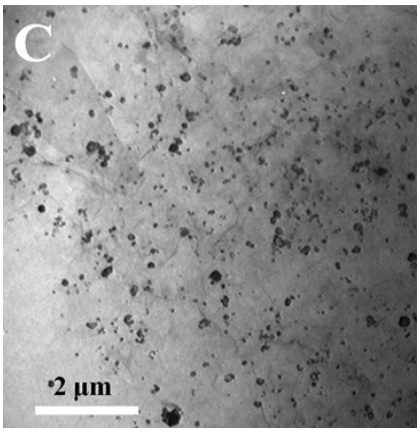

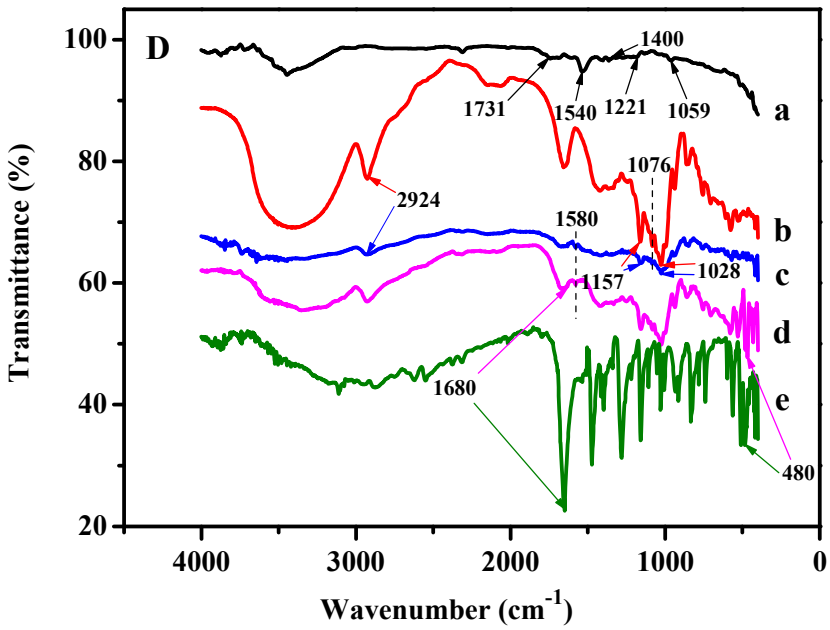

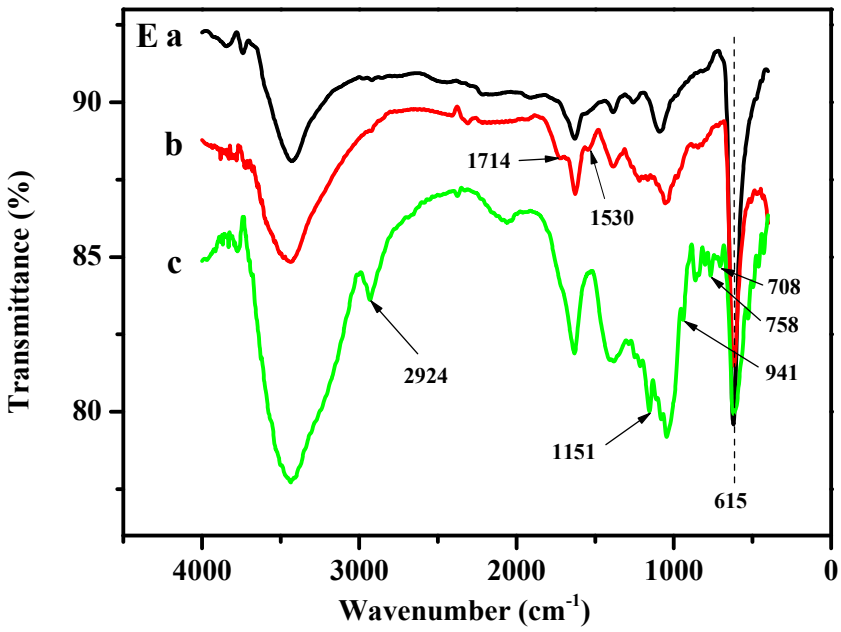

Fig. 2

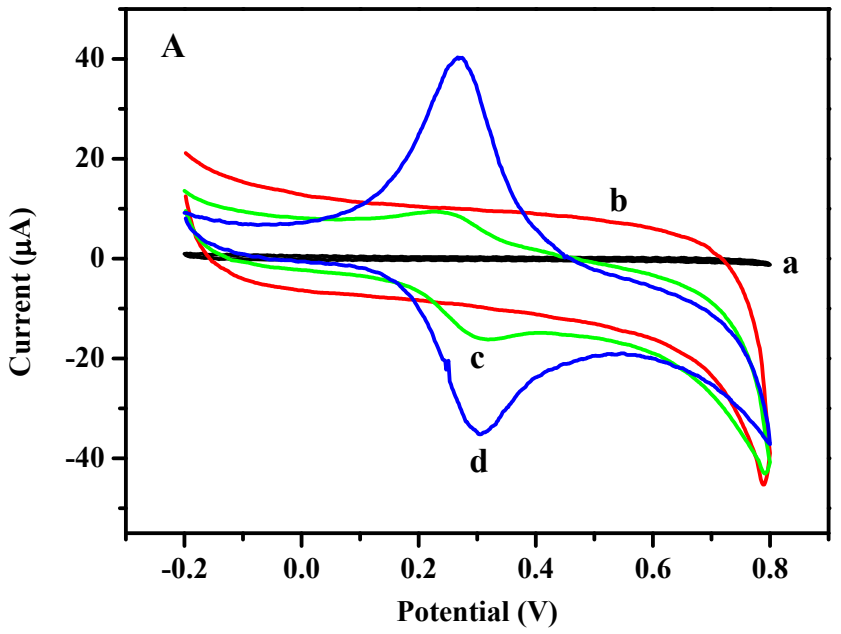

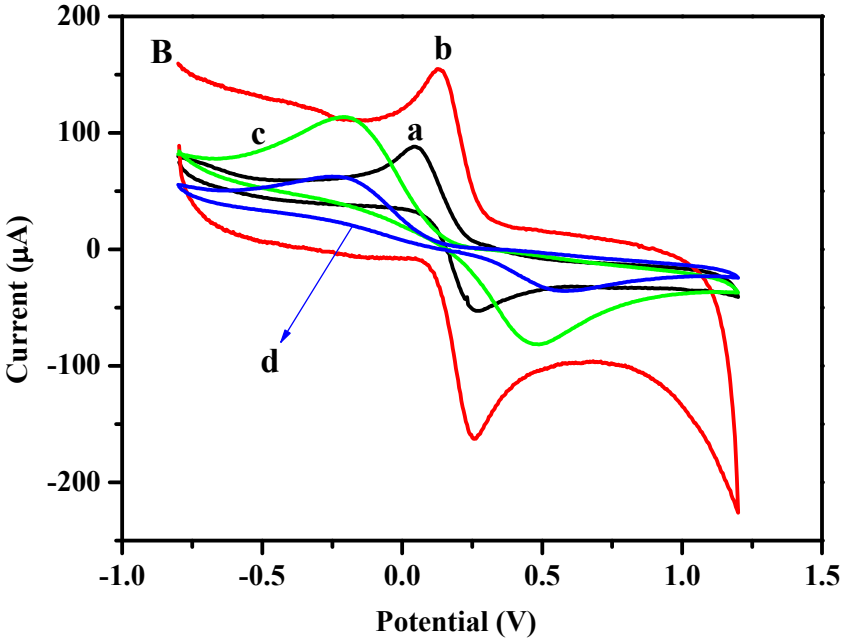

Fig. 3

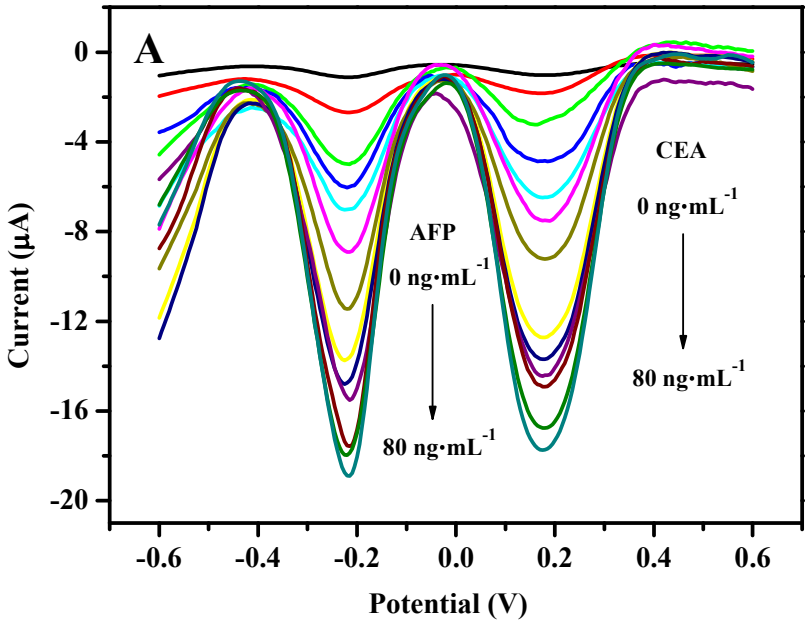

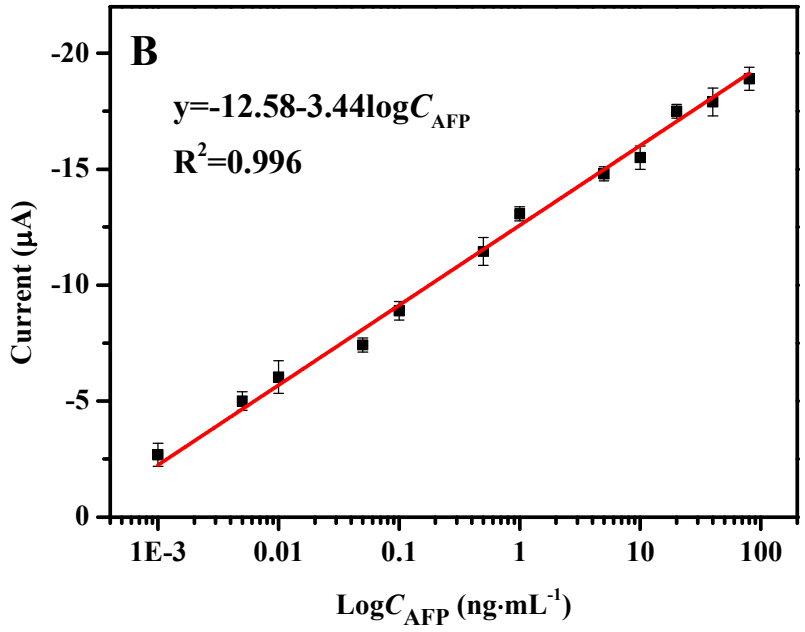

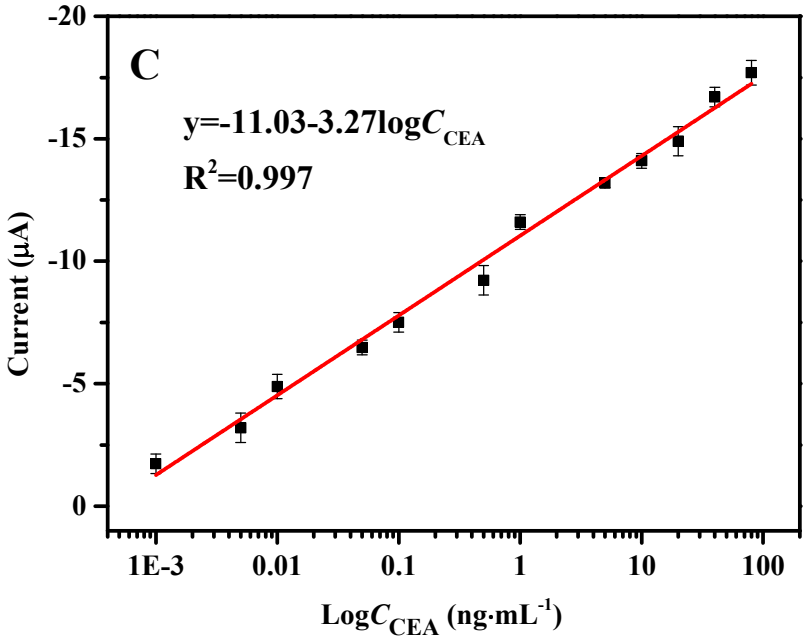

Fig. 4

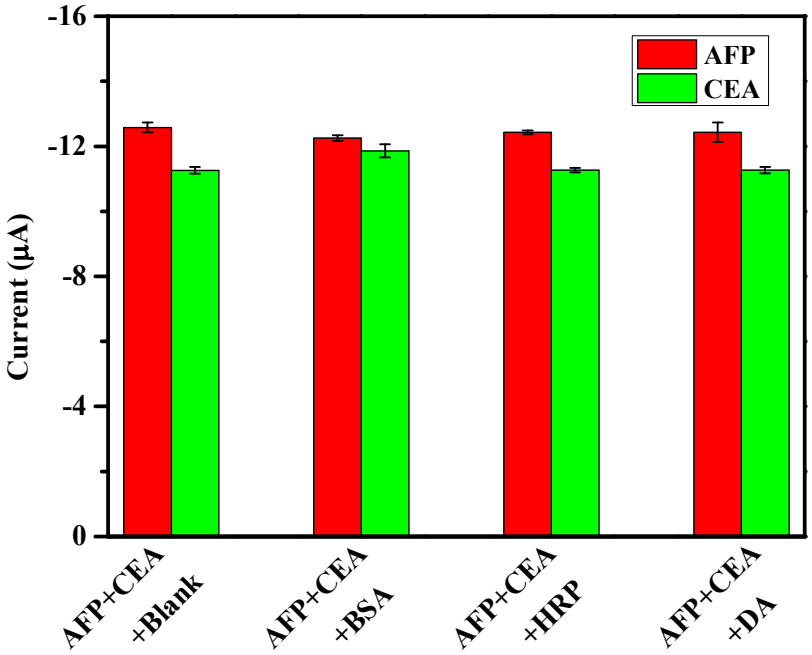

Table 1

Sample NO.	Content (ng·mL^{-1})		Added CEA (ng·mL^{-1})		Founded CEA (ng·mL^{-1})		Recovery (%)		RSD (%, n=5)	
	CEA	AFP	CEA	AFP	CEA	AFP	CEA	AFP	CEA	AFP
1	0.5	0.5	5.0	5.0	5.4	5.6	98.2	101.8	3.5	3.7
2	1.0	1.0	10.0	10.0	11.2	10.8	101.8	98.2	4.6	3.3
3	2.0	2.0	15.0	15.0	16.9	16.8	99.4	98.8	2.8	2.8
4	5.0	5.0	20.0	20.0	24.8	25.8	99.2	103.2	3.2	5.2
5	10.0	10.0	25.0	25.0	35.1	35.3	100.3	100.9	2.4	2.1

Graphical Abstract:

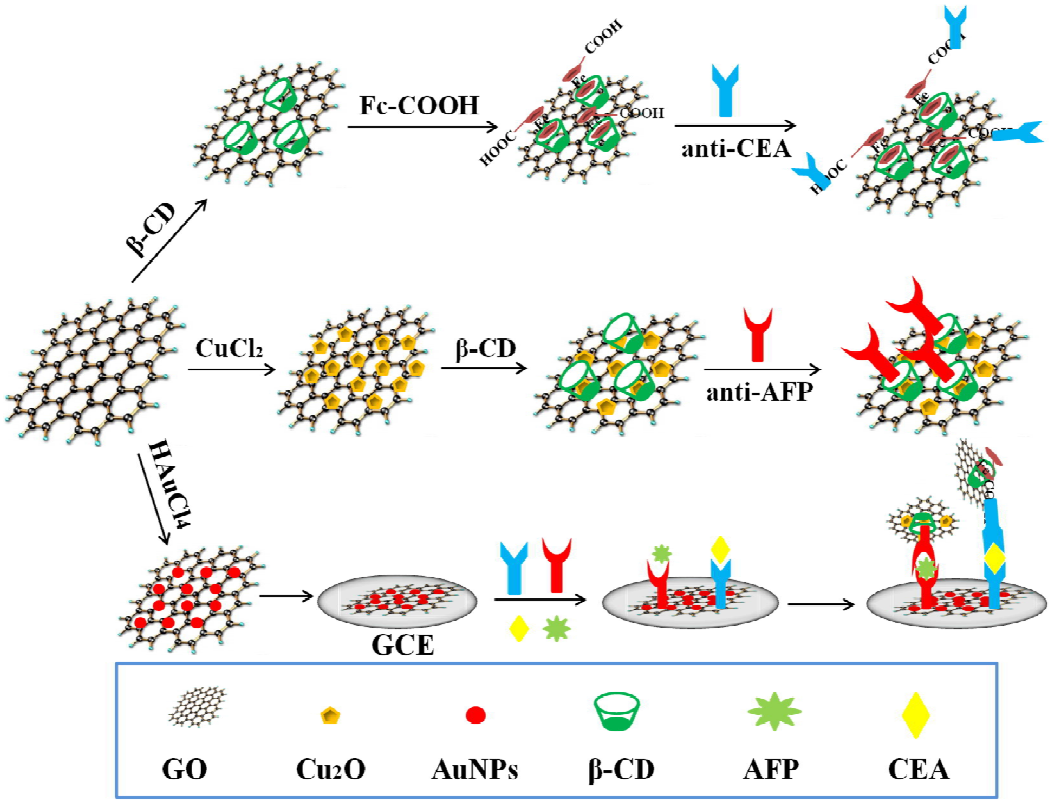

An electrochemical immunosensor was developed using GO-AuNPs as substrate, Cu_2O-GO-CD and GO-CD-Fc as probes, and showed excellent electrochemical performances.